

PHOSPHORUS AND CHLOROPHYLL DEGRADATION PRODUCT PROFILES IN SEDIMENT FROM REELFOOT LAKE, TENNESSEE

JOHN PARDUE¹, DAVID H. KESLER, JEAN DABEZIES² AND LEE PRUFERT³
Rhodes College
Memphis, Tennessee 38112

ABSTRACT

Total phosphorus and chlorophyll degradation product profiles were determined in short sediment cores from Reelfoot Lake, Tennessee in May 1981, and February and October, 1983. There was no relationship between total phosphorus and chlorophyll degradation product profiles within these cores. Total phosphorus profiles from homogenized, incubated cores did not develop surface maxima. These data are discussed in light of Carignan and Flett's (1981) observation of phosphorus post-depositional migration.

INTRODUCTION

From the results of a straightforward lab experiment, Carignan and Flett (1981) demonstrated that total phosphorus sediment profiles may be of little use in determining historical phosphorus levels or phosphorus sedimentation rates. Their conclusion was based upon the development of a total phosphorus maximum in the upper 1 cm of previously homogenized sediment. We felt Carignan and Flett's hypothesis of phosphorus remobilization could be further tested if there existed a commonly measured substance that was deposited with phosphorus but did not migrate upward in the reduced zone. Sedimentary chlorophyll degradation products (SCDP's) were chosen because they are stable, correlate well with trophic levels (Sanger and Gorham, 1972), are assumed not to migrate, and have been used to estimate historical changes in lacustrine phytoplankton populations (Staub, 1978). We also wanted to determine the phosphorus remobilization rate. To achieve this, an experiment was performed twice using previously homogenized sediment cores which were incubated for different lengths of time.

METHODS

Short sediment cores were taken from the Lower Blue Basin of Reelfoot Lake (36 25'N, 89 22'W), Tennessee. The surface area of the lake is 465 ha with an average depth of 1.8 m. Reelfoot Lake is hypereutrophic and large portions of the lake, other than the lower Blue Basin, are choked with aquatic macrophytes (W. Smith, pers. comm.).

One core, taken on 9 May 1981, was returned to Memphis in an upright position and frozen. Sections (1 or 2 cm) were then cut as the core was extruded. Two cores were taken on 12 February 1983 and five additional cores were taken on 7 October 1983. One core from each of the February and October sampling dates was sectioned immediately in the field using a modified technique ideal for

unconsolidated sediments like those found at Reelfoot Lake. The apparatus for this technique is shown in Figure 1. Sections, 1 or 2 cm, were extruded and drained immediately into sample bottles. The remaining cores (20-32 cm long) were homogenized in the lab by vigorous shaking and by stirring with a glass rod. These homogenized cores

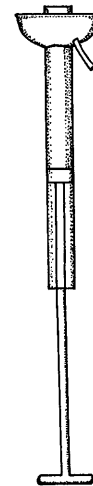


FIG. 1. Core extraction device used to collect unconsolidated sediment.

were kept vertical at 8 C in the dark before sectioning and analysis. A 10-12 cm layer of water was maintained over the top of the cores. Air was constantly bubbled into the water above the sediment. The homogenized core from 12 February was sectioned after 28 days. The three remaining cores from 7 October were sectioned after 10, 53, and 60 days, respectively.

SCDP's were extracted from 1-2 g sub-samples of the sections with 30 ml of 90% basic acetone and 5% dimethylaniline by the method described by Wetzel and Likens (1979). The standard Sedimentary Chlorophyll Degradation Unit (SCDU), defined by Vallentyne (1955), is the optical density with a 1 cm light path at the wavelength of maximum absorbance in the red end of the spectrum from the baseline absorbance at 750 nm. The optical density of the SCDP extract was determined immediately using a Gilford 2600 spectrophotometer.

Sub-samples were taken for dry-weight (DW) and ash-free dry weight (AFDW) determinations (Taras, et al., 1975). Total phosphorus (TP) concentrations were determined by crushing the ashed samples with a mortar and pestle and boiling for 10 minutes in 0.2 N HCl. The resulting solution was filtered through Whatman GF/C filters, followed by distilled water rinses. Soluble reactive phosphorus of the filtrate was determined by the molybdate-antimonyl-ascorbic acid method of Strickland and Parsons (1972). Triplicate assays were performed on each sample

¹Present address: Lab for Wetland Soils and Sediments, Louisiana State University, Baton Rouge, LA 70803

²Present address: Louisiana State University Medical School, New Orleans, LA 70112

³Present address: Geology Department, University of North Carolina, Chapel Hill, North Carolina 27514

and 2-3 samples were analyzed for each depth.

RESULTS AND DISCUSSION

The SCDP concentrations ($SCDU \cdot gm DW^{-1}$) from the field (sectioned immediately after sampling) and homogenized cores are given in Figures 2-5. TP data are expressed as $ug P \cdot g AFDW^{-1}$ and are given in Figures 6-8.

The SCDP concentrations observed here were within the range of values reported for other lakes (Valentyne 1955; Gorham, 1961; Sanger and Gorham, 1972; Whitehead et al., 1973; D. Culver, pers. comm.). The 1981 SCDP concentrations (Figure 2) were similar to the 1983 cores (Figure 3), although the profile of the 1981 core showed no consistent decrease with depth. In both 1983 field cores, SCDP concentrations approximately tripled from the bottom to the top of the cores. However, these data, collected in November and February, are different in both profile shape and absolute values. These differences could have been due to small changes in sampling site or seasonal variation. A more rigorous sampling program could resolve this question. Freezing of the 1981 core caused it to lengthen and probably distorted the upper layers. In both 1983 field cores, maxima were observed within the top two cm. This was due to epipellic production and/or sedimentation of phytoplankton. The overall increase seen in both cores is probably due to increased production over time as the lake has become more eutrophic. Until sedimentation rate data are collected this question cannot be answered.

The data from the February 1983 homogenized core (Figure 4) demonstrated the same general decline in SCDP concentration with depth as seen in the field core. Because homogenization of the core was vigorous, this profile was probably determined by differential sorting as the material settled. A process of sediment resuspension followed by sorting is probably occurring in the lake during the winter. These sediments were fluid and the long fetch of the wind

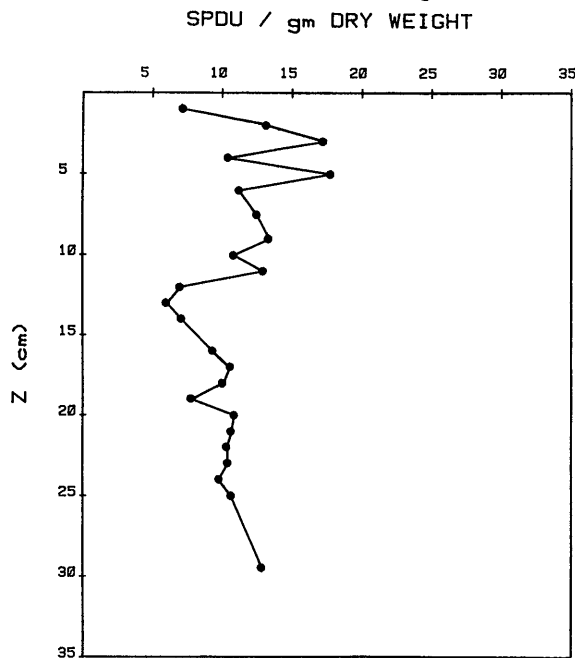


FIG. 2. SCDP concentration ($SCDU \cdot gm DW^{-1}$) versus Depth (cm) from a core taken on May 9, 1981 at depth of five meters in Blue Basin, Reelfoot Lake.

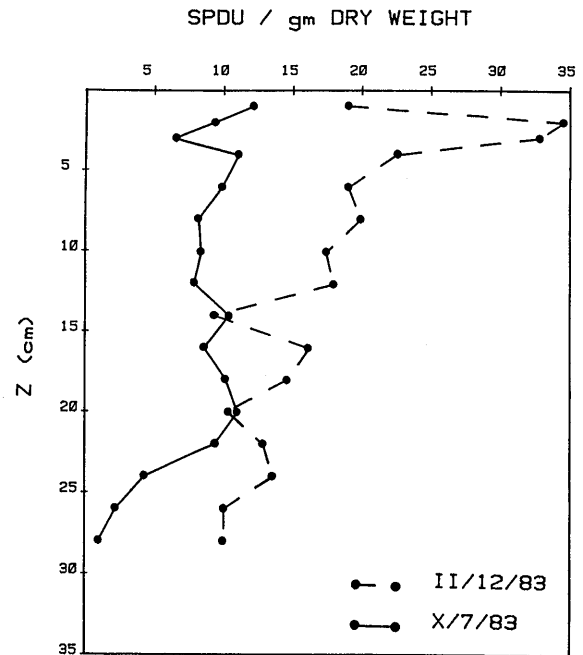


FIG. 3. SCDP concentration ($SCDU \cdot gm DW^{-1}$) versus Depth (cm) from cores taken on February 12, 1983 and October 7, 1983 in Blue Basin, Reelfoot Lake.

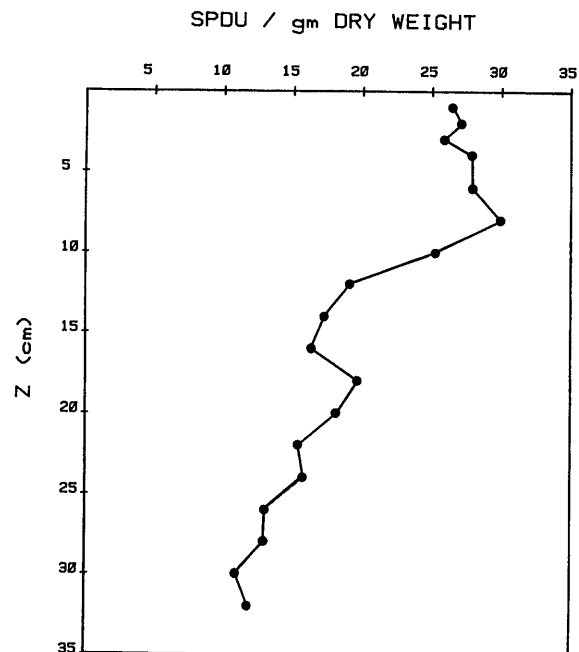


FIG. 4. SCDP concentration ($SCDU \cdot gm DW^{-1}$) versus Depth (cm) from a core taken on February 12, 1983 at a depth of five meters in Blue Basin, Reelfoot Lake and homogenized before sectioning.

on the shallow lake may have been able to resuspend these. The data from the October 1983 homogenized cores did not show the general decrease in SCDP concentration with depth. The high surficial SCDP concentration after 60 days of incubation was probably due to epipellic production. While the cores were kept in a darkened, constant-

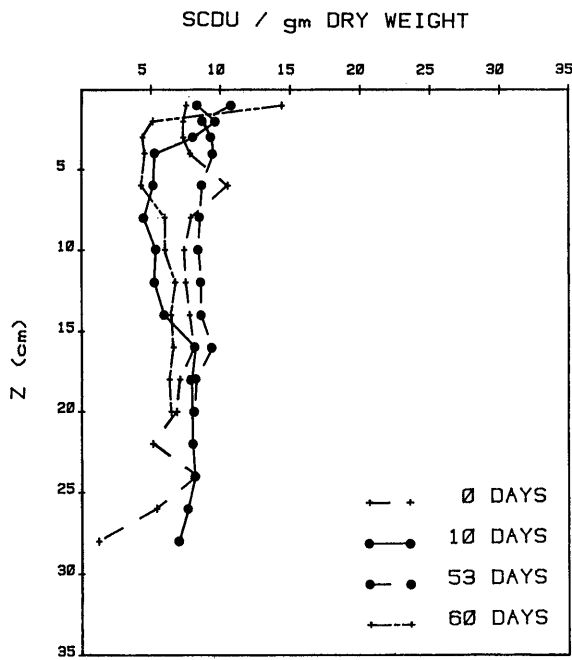


FIG. 5. SCDP concentration (SCDU \bullet gm DW⁻¹) versus Depth (cm) from cores taken on October 7, 1983 that were homogenized and incubated for 0, 10, 53, and 60 days before sectioning.

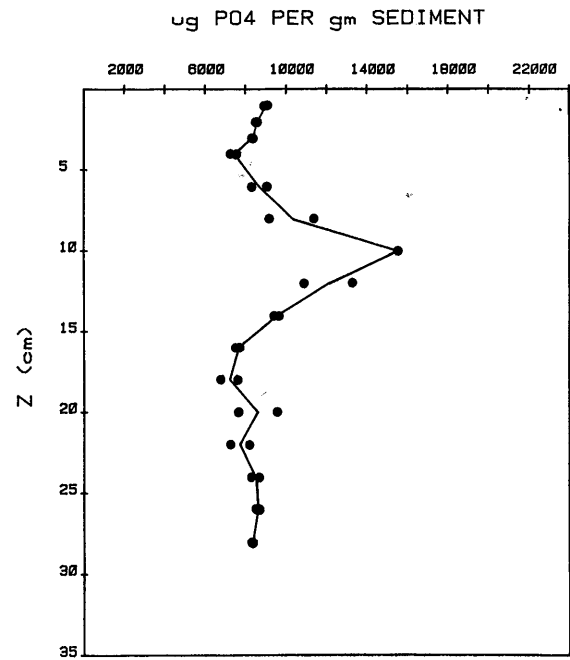


FIG. 7. TP concentration (μ g Total Phosphorus \bullet gm AFDW⁻¹) versus Depth (cm) from a core taken on October 7, 1983 in Blue Basin, Reelfoot Lake.

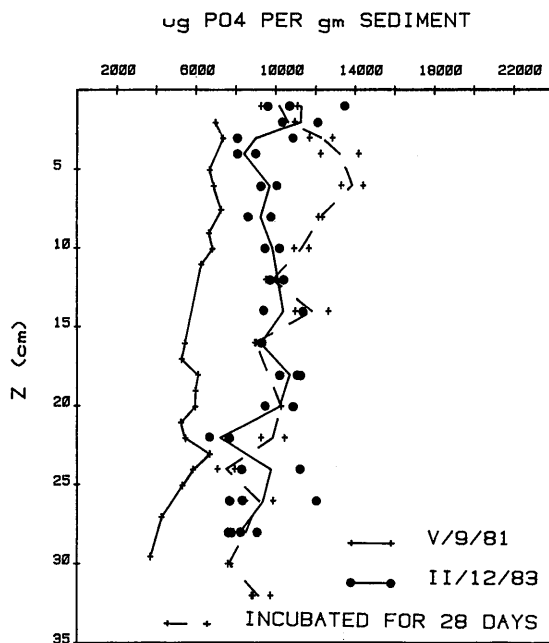


FIG. 6. TP concentration (μ g Total Phosphorus \bullet gm AFDW⁻¹) versus Depth (cm) from cores taken on May 9, 1981 and February 12, 1983 in Blue Basin, Reelfoot Lake. The remaining core was collected on February 12, 1983, homogenized and incubated for 28 days before sectioning.

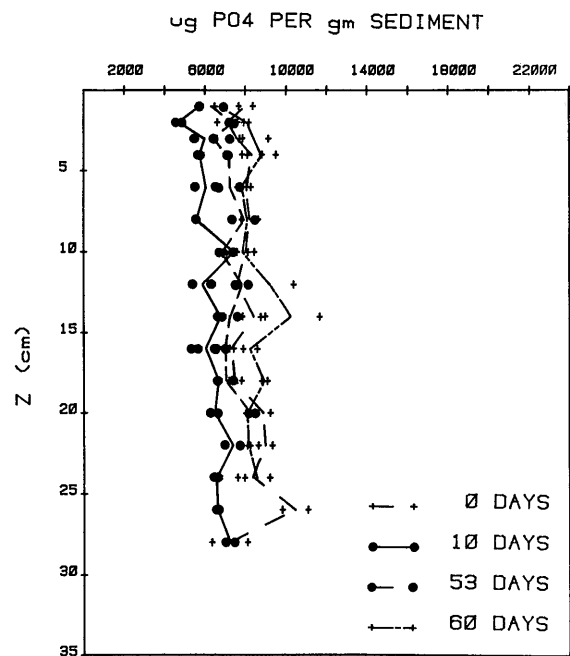


FIG. 8. TP concentration (μ g Total Phosphorus \bullet gm AFDW⁻¹) versus Depth (cm) from cores taken on October 7, 1983 in Blue Basin, Reelfoot Lake that were homogenized and incubated for 0, 10, 53, and 60 days before sectioning.

temperature room, dim light occasionally reached the cores possibly supporting epipelagic algal growth (P. Rich, per. comm.). Nevertheless, we did not observe development of a consistent SCDP profile in the cores incubated for 10, 53, or 63 days (see Figure 5).

The TP concentrations from the 1981 core (Figure 6) showed a steady decrease with depth. The shape of the profile from this core was similar to that seen in the February 1983 core, although the concentrations were lower.

The TP profile from the February 1983 core did not demonstrate a definite maximum. The October core (see Figure 7), while having similar TP values in the top 5 and bottom 10 cm, displayed a maximum at 10 cm. The homogeneous profile seen in February suggests to us that the sediments were mixed to at least 10 cm before the February core was taken.

When our values are converted to a dry weight basis, they are similar to those reported by Edmondson (1974) for Lake Washington before sewage addition, and to other short sediment cores (Fish and Andrew, 1980; Yoshida, 1981; Carignan and Flett, 1981, (2.5 m station); D. Brenner, pers. comm.). Phosphorus concentrations in six Wisconsin lakes were much higher than our converted data from Reelfoot Lake (Bortleson and Lee, 1974).

The TP profile that developed in the core collected in February 1983 and incubated for 28 days (Figure 6) showed similar TP concentrations in the top few and bottom 15 cm, but diverged from the field core's profile between 3 and 10 cm. Like the SCDP data from the same 28-day incubated core suggested, there may have been either sorting of material upon settling or postdepositional migration. The TP profiles that developed in the homogenized October cores (Figure 8) remained straight. Because incubation conditions were the same in February and October, the divergence of the core incubated in February from the cores incubated in October was not due to postdepositional migration of phosphorus but to sorting differences.

We did not observe profiles in incubated cores that resembled those reported by Carignan and Flett (1981). The TP values from the first experiment (28-day incubation) showed a maximum in the 5-6 cm section, but this was too deep to be explained by remobilization. In the second experiment, no surficial TP maximum developed in any of the three incubated cores.

There were no TP maxima near the sediment surface as seen by Carignan and Flett (1981) which would suggest

redeposition of phosphorus. Our data suggest that any post-depositional migration of phosphorus occurring in Reelfoot Lake is being masked by resuspension and sorting of sediments during wind-driven circulation. Our inability to observe a TP maximum may have been due to insufficient incubation time and/or lack of precision necessary to observe a maximum within a narrow depth range. Likewise, sediment type can affect phosphorus movement (Holden and Armstrong, 1980; Bostrom and Peterson, 1982).

There were no relationships between the TP and SCDP profiles in the field cores. These data indicate that TP and SCDP assorted independently within the sediments. However, the orthograde TP and SCDP profiles of the incubated cores neither support or refute the hypothesis that TP and SCDP assort independently.

REFERENCES CITED

- Bortleson, G.C. and G.F. Lee. 1974. Phosphorus, iron, and manganese distribution in sediment cores of six Wisconsin Lakes. *Limnol. Oceanogr.* 19:794-801.
- Bostrom, B. and K. Petterson. 1982. Different patterns of P release from Lake sediments in laboratory experiments. *Hydrobiologia* 92:415-429.
- Carignan, R. and R.J. Flett. 1981. Post-depositional mobility of phosphorus in lake sediments. *Limnol. Oceanogr.* 26:361-366.
- Edmondson, W.T. 1974. The sedimentary record of the eutrophication of Lake Washington. *Proc. Nat. Acad. Sci.* 71:5093-5095.
- Fish, G.R. and I.A. Andrew. 1980. Nitrogen and phosphorus in the sediments of Lake Rotoura. *New Zea. J. Mar. Fresh. Res.* 14:121-128.
- Gorham, E. 1961. Chlorophyll derivatives, sulphur, and carbon in cores from two English lakes. *Can. J. Bot.* 39:333-338.
- Holdren, G.C. and D.E. Armstrong. 1980. Factors affecting phosphorus release from intact lake sediment cores. *Environ. Sci. Technol.* 14:79-87.
- Sanger, J.E. and E. Gorham. 1972. Stratigraphy of fossil pigments as a guide to the postglacial history of Kirchner Marsh, Minnesota. *Limnol. Oceanogr.* 17:840-854.
- Staub, E. 1978. Stratigraphy of diatoms and chlorophyll derivatives in the uppermost sediment of a Swiss lake. In, *Interactions between Sediments and Freshwater*. Golterman, H.L. (ed.). The Hague: Junk, 161-164.
- Strickland, J.D.H. and T.R. Parsons. 1972. A practical handbook of seawater analysis. *Fish. Res. Bd. Can. Bull.* 167.
- Taras, M.J., A.E. Greenburg, R.D. Hoak, and M.C. Rand (eds.). 1971. *Standard Methods for the Examination of Water and Wastewater*. Amer. Publ. Health Assoc. Washington, D.C. 873pp.
- Vallentyne, J.R. 1955. Sedimentary chlorophyll determination as a paleobotanical method. *Can. J. Bot.* 33:304-313.
- Wetzel, R.G. and G.E. Likens. 1979. *Limnological Analyses*. W.B. Saunders Co. 357pp.
- Whitehead, D.R., H. Rochester, Jr., S.W. Rissing, C.B. Douglass, and M.C. Sheehan. 1973. Late glacial and post-glacial productivity changes in a New England pond. *Science* 181:744-747.
- Yoshida, T. 1981. Mathematical model of phosphorus release from lake sediment. *Verh. Internat. Verein. Limnol.* 21:268-274.

JOURNAL OF THE TENNESSEE ACADEMY OF SCIENCE

VOLUME 61, NUMBER 2, APRIL, 1986

ADDITIONS TO THE KNOWN VASCULAR FLORA OF LAND BETWEEN THE LAKES, 1. NEW DICOT RECORDS

EDWARD W. CHESTER
Austin Peay State University
Clarksville, Tennessee 37040

ABSTRACT

One-hundred and five dicot species are added to the floristic list for Land Between the Lakes, a 170,000-acre conservation, education, and recreation facility managed by the Tennessee Valley Authority in western Kentucky and Tennessee.

INTRODUCTION

Land Between the Lakes (LBL), a 170,000-acre tract in southwestern Kentucky and northwestern Middle Tennessee, has been managed since 1964 by the Tennessee Valley Authority as a public conservation, education, and recreation facility. The area encompasses parts of Lyon and

Trigg counties in Kentucky and Stewart County in Tennessee. It is bounded on the west by Kentucky Lake (impounded Tennessee River), on the east by Barkley Lake (impounded Cumberland River), and on the north by a man-made canal connecting the two lakes. The southern boundary has no natural or man-made demarcation; only survey lines and markers separate LBL from private holdings.

Some alluvial bottomlands and wetlands adjoin the rivers and their major tributaries but most of LBL consists of rolling to steeply-dissected uplands. The secondary, mostly oak-hickory forests which cover about 75 percent of the area are, with the exception of some ecologically significant sites, periodically and selectively harvested. Some bottomlands are leased to area farmers for cultivation and many fields once devoted to agricultural practices are maintained and managed for wildlife. Otherwise, lands formerly occupied by farmsteads, homes, and communities are now in various successional stages. The numerous educational, recreational, and historical features developed by TVA attract an increasing number of visitors.

Ellis *et al.* (1971) made a preliminary survey of the LBL flowering plants during the early and middle 1960's and identified 799 taxa, including 136 introductions. Additions by Chester *et al.* (1976), Ramsey and Chester (1981), Chester (1982, 1984), and the present report bring the total list to 942, including 757 native and 186 introduced taxa.

METHODS

Work toward an annotated account of the LBL vascular flora continues out of Austin Peay State University. Pursuant to completion of that study, which will document the significance and relationships of the flora and address changes resulting from public ownership and TVA management, many species have been and continue to be added to the LBL list. In many cases, these need to be made available to those interested in the Tennessee and Kentucky flora. This paper reports 105 dicot species (65 native and 40 introductions) not previously listed for LBL and is based mainly upon my collections since 1971. Other groups will be included in subsequent reports.

The present list includes a mixture of native species, pre-public ownership introductions, and in a few cases, recent introductions. Collection data are not included to conserve space but all specimens cited are vouchered at APSU. A brief annotation for each species provides the habitat in which that plant has been most often observed in LBL. Families are listed alphabetically; nomenclature follows Cronquist (1980) for composites and mostly Fernald (1950) for others except for those groups annotated by specialists. These include: *Amaranthus* (J. D. Sauer), *Callitriche* and *Myriophyllum* (David Webb), *Ptilimnium* (John Thieret), *Thaspium* and *Zizia* (Anne H. Lindsey), *Trepocarpus* (John Thieret and R. Dale Thomas), and *Vernonia* (Sam Jones). As in previous reports, county distributions are indicated by L and T for Lyon and Trigg counties and S for Stewart County. Introduced species are denoted by an asterisk.

LIST OF SPECIES

AMARANTHACEAE

Amaranthus tuberculatus (Moq.) Sauer. Mudflats of both lakes (L,S,T).

APIACEAE

Ptilimnium nuttallii (DC) Britt. Sandy shores of Kentucky Lake (S,T).

Thaspium pinnatifidum (Buckl.) Gray. Edges of oak-hickory woodlands (T).

Thaspium trifoliatum (L.) Gray. Mesic woodlands (L,S,T).

Trepocarpus aethusae Nutt. Sandy shores of Kentucky Lake (L,S,T).

Zizia aptera (Gray) Fern. Mesic, open woodlands (S,T).

ASTERACEAE

**Artemisia vulgaris* L. Open roadsides (S).

Aster simplex Willd. Mudflats, riverine marshes (S,T).

Bidens cernua L. Mudflats, swamps (L,S,T).

**Centaurea cyanus* L. Open, weedy roadsides (S).

**Chrysopsis camporum* (Greene) Shinn. Roadsides, fields (S).

Conyza ramosissima Cronq. Abandoned gravel driveways (S).

**Coreopsis lanceolata* L. Roadsides and homesites (S,T).

Erigeron pulchellus Michx. Shaded banks, open woods (S).

Eupatorium altissimum L. Fields, open roadsides (S).

Eupatorium incarnatum Walt. Ditches, wet woodlands (S).

Eupatorium perfoliatum L. Mesic fields and thickets (L,S,T).

Eupatorium sessilifolium L. Dry thickets, open fields (L,S).

Helianthus angustifolius L. Dry fields, open woods (L,S,T).

**Helianthus annuus* L. Fields and roadsides (S).

Helianthus atrorubens L. Dry, weedy fields and roadsides (S).

Helianthus occidentalis Ridd. Dry fields, open woods (T).

Helianthus tuberosus L. Alluvial thickets, creekbanks (S,T).

**Iva annua* L. Dry fields and roadsides, bottomlands (L,S,T).

Krigia oppositifolia Raf. Fallow fields, sandy shores (L,S,T).

Kuhnia eupatorioides L. Dry fields and roadsides (T).

Mikania scandens (L.) Willd. Thickets along Kentucky Lake (S).

Pluchea camphorata (L.) DC. Swamps, wet fields (L,S,T).

Preanthes barbata (T. & G.) Milst. Dry woods, thickets (S).

Rudbeckia laciniata L. Low thickets (S,T).

Silphium astericus L. Dry fields and thickets (T).

Solidago altissima L. Mesic thickets, fields (L,S,T).

Solidago gigantea Ait. Mesic fields and roadsides (S).

Solidago hispida Muhl. Dry, open woods (L,S).

Solidago rugosa Mill. Mesic, weedy fields (S).

Solidago ulmifolia Muhl. Dry forest borders, open woods (L,S,T).

Vernonia gigantea (Walt.) Trel. Mesic fields, thickets (L,S,T).

BERBERIDACEAE

**Berberis thunbergii* DC. Homesites (T).

BORAGINACEAE

**Lithospermum arvense* L. Open roadsides, fields (T).

BRASSICACEAE

**Brassica rapa* L. Roadsides, meadows (L,S,T).

**Lepidium campestre* (L.) Brown. Fields, homesites (S).

**Thlaspi arvense* L. Open roadsides (T).

CALLITRICHACEAE

Callitriche deflexa A. Browne. Spring branches (S).

CAPRIFOLIACEAE

**Lonicera X bella* Zabel. Homesites (S).

CARYOPHYLLACEAE

**Agrostemma githago* L. Fields and roadsides (S).

Arenaria patula Michx. Open, sandy fields and roadsides (T).

**Arenaria serpyllifolia* L. Open, sandy fields and roadsides (S,T).

**Cerastium viscosum* L. Fallow bottomland fields (L,S,T).

**Cerastium vulgatum* L. Fallow fields, meadows, roadsides (L,S,T).

**Holosteum umbellatum* L. Roadsides, meadows (L).

Paronychia fastigiata (Raf.) Fern. Dry, wooded slopes (T).

Sagina decumbens (Ell.) T. & G. Sandy fields, paths (L).

EUPHORBIACEAE

Crotonopsis elliptica Willd. Dry, sandy roadbanks (S).

**Euphorbia cyparissias* L. Spreading around homesites (T).

**Euphorbia marginata* Pursh. Spreading around homesites (S).

Phyllanthus carolinensis Walt. Mudflats, sandy fields (L,S,T).

FABACEAE

Astragalus canadensis L. Sandy banks of Kentucky Lake (S).

Desmanthus illinoensis (Michx.) MacM. Riverbanks (S,T).

Desmodium ciliare (Muhl. ex Willd.) DC. Dry fields (L,S,T).

Desmodium sessilifolium (Torr.) T. & G. Dry fields (T).

Lespedeza capitata Michx. Barrens (S).

Lespedeza repens (L.) Bart. Dry fields and roadsides (L,S,T).

**Lespedeza stipulacea* Maxim. Fields and meadows (S).

**Lespedeza striata* (Thunb.) H. & A. Fields and meadows (S).

**Medicago lupulina* L. Roadsides, cemeteries, homesites (L,S,T).

**Trifolium dubium* Sibth. Fields, cemeteries (L,T).

**Trifolium, hybridum* L. Meadows, old lawns (S).

**Vicia angustifolia* Reich. Roadsides, thickets (L,T).

**Vicia villosa* Roth. Thickets, fields, homesites (L,S,T).

FAGACEAE

**Quercus acutissima* Carruth. Planted for mast crops (T).

HALORAGACEAE

**Myriophyllum spicatum* L. Shallow embayment, Lake Barkley (L).

HYDROPHYLLACEAE

Hydrophyllum appendiculatum Nutt. Mesic woodlands (S,T).

LAMIACEAE

- Collinsonia canadensis* L. Mesic woodlands (L,S,T).
Isanthus brachiatus (L.) BSP. Sandy roadsides, slag dumps (L,T).
 **Marrubium vulgare* L. Homesites (S).
 **Nepeta catarica* L. Homesites (T).
 **Physostegia virginiana* (L.) Benth. Homesites, fields (S).
Pycnanthemum virginianum (L.) Dur. & Jack. Dry roadsides and prairie remnants (S,T).
Scutellaria integrifolia L. Wet fields and thickets along Kentucky Lake (S).

ONAGRACEAE

- Jussiaea leptocarpa* Nutt. Sandy banks of lakes and streams (S).
Jussiaea repens L. var. *glabrescens* Kunth. Swamps, ditches (S,T).
 **Jussiaea uruguayensis* (Camb.) Hara. Open marshes in Cumberland River bottomlands (S).

OROBANCHACEAE

- Conopholis americana* (L.) Wallr. Mesic woodlands (S).

PLANTAGINACEAE

- Plantago pusilla* Nutt. Sandy fields, cemeteries (L,T).
Plantago rugelii Dcne. Meadows, homesites, roadsides (L,S,T).

POLYGONACEAE

- **Polygonum aviculare* L. Sandy fields, gravel roads (L,S,T).
 **Polygonum cespitosum* Blume var. *longisetum* (DeB.) Stew. Ditches, wet fields, homesites (L,S,T).
 **Polygonum cuspidatum* Sieb. & Zucc. Homesites (S).
Polygonum sagittatum L. Low thickets and fields (S).
Rumex altissimus Wood. Sandy lakeshores (S,T).

PRIMULACEAE

- **Lysimachia nummularia* L. Wet fields, ditches (S,T).

RANUNCULACEAE

- Myosurus minimus* L. Fallow bottomland fields (S,T).
 **Ranunculus parviflorus* L. Pond margins, wet fields (S,T).
Ranunculus fascicularis Muhl. Dry, open woods (T).
 **Ranunculus sardous* Crantz. Bottomlands (L,S,T).

- Thalictrum dioicum* L. Mesic, wooded slopes (T).

ROSACEAE

- Agrimonia rostellata* Wallr. Wooded slopes and ravines (L,S,T).

SALICACEAE

- **Populus nigra* L. Spreading around homesites (T).

SCROPHULARIACEAE

- Buchnera americana* L. Dry, open fields and roadsides (T).
Chelone glabra L. Mesic thickets, streambanks (S).
Penstemon australis Small. Dry woods, roadbanks (S).
Penstemon calycosus Small. Mesic woods, roadsides (S).
Veronica peregrina L. Fallow bottomland fields (S,T).
 **Veronica serpyllifolia* L. Moist meadows, old lawns (L,S).

VALERIANACEAE

- Valeriana pauciflora* Michx. Alluvial forests (S).

LITERATURE CITED

- Chester, E. W., L. J. Schibig, and R. J. Jensen. 1976. The woody flora of Land Between the Lakes, Kentucky and Tennessee. *Journ. Tenn. Acad. Sci.* 51:124-129.
 ———. 1982. Some new distributional records for *Lesquerella lescurei* (Gray) Watson, including the first report for Kentucky. *Sida* 9:235-237.
 ———. 1984. Notes on the vascular flora of Tennessee, particularly of the northwest Highland Rim, II. *Journ. Tenn. Acad. Sci.* 59:50-52.
 Cronquist, A. 1980. Vascular flora of the Southeastern United States, Vol. 1. Asteraceae. Univ. North Carolina Press, Chapel Hill. 261 p.
 Ellis, W. H., E. Wofford, and E. W. Chester. 1971. A preliminary checklist of the flowering plants of Land Between the Lakes. *Castanea* 36:229-246.
 Fernald, M. L. 1950. Gray's manual of botany, 8th edition. American Book Co., New York. 1632 p.
 Ramsey, G. W., and E. W. Chester. 1981. The occurrence of *Cimicifuga rubifolia* Kearney in the Interior Low Plateaus of Tennessee. *Castanea* 46:100-101.

JOURNAL OF THE TENNESSEE ACADEMY OF SCIENCE

VOLUME 61, NUMBER 2, APRIL, 1986

POSSIBLE MARGIN OF THE REELFOOT RIFT IN STEWART COUNTY, TENNESSEE

GAIL A. NIXON AND PHILLIP R. KEMMERLY
 Austin Peay State University
 Clarksville, Tennessee 37044

ABSTRACT

A preliminary study of the aeromagnetic data from the Tharpe and Standing Rock quadrangles suggests that the east boundary of the Reelfoot rift passes near two prominent magnetic highs in the area. Second derivative mapping by Vacquier's technique reveals two asymmetric bodies, each approximately 19.5 km in length. Analysis of maximum depth to the magnetic basement by Peters half-slope method and Vacquier vertical prisms indicates a relief of 0.5 km between the two anomalies, with the north (Tharpe) anomaly at a depth of 3.0 km. These depths are confirmed by data on established margins of the rift to the southwest. The two anomalies probably represent plutons associated with a down-dropped block, part of a normal fault zone bordering the Reelfoot rift.

INTRODUCTION

Aeromagnetic maps of the Stewart County, Tennessee area indicate two distinct, neighboring magnetic regions of high intensity. They occur on the Kentucky-Tennessee border, at latitude 36°30'N, longitude 88°W (Figure 1).

This paper analyzes these regions for the purpose of postulating the structural features that are responsible for the contrast in magnetic signatures, and their possible link to the southeastern margin of the Reelfoot rift.

MAGNETIC ANALYSIS

Residual total intensity aeromagnetic maps (scale 1:125,000) of the region show two anomalies. The southernmost anomaly, in the Standing Rock quadrangle, is a more intense magnetic high with a relief of 600 gammas. The second anomaly occurs in the Tharpe quadrangle and exhibits a 350-gamma magnetic relief.

Several magnetic profiles of the two anomalies were drawn from the map contours. The profile A-A' passes through both anomalies on the average perpendicular to the steepest magnetic gradient (Figures 1 & 2). The steepest slopes on both profiles are themselves inversely related to the depth to the top of the anomalies (Vacquier and others, 1951). Half-slope analysis of the depth to the magnetic basement (after Peters, as described in Nettleton, 1976) averaged 3-km depth in the Tharpe area and up to 2.6 km in the Standing Rock quadrangle. To substantiate these depth estimates, another analysis was done using Vacquier's vertical prism-horizontal gradient comparison method (Vacquier and others, 1951). In applying Vacquier's method, the Tharpe anomaly was referenced to a 1 × 6 model and Standing Rock to a 4 × 6 model based on a comparison of the shapes of the magnetic contour closures with Vacquier's reference figures. The horizontal extent and location of maximum gradient on each anomaly led to

appropriate "depth indices". Calculated depths for the Tharpe and Standing Rock anomalies were, respectively, 2.9 km and 2.5 km. These depths agree with Hildenbrand's basement depth estimates for the general region (Hildenbrand, 1982).

To delineate the shape, size, and orientation of the source of the magnetic anomalies, a second derivative, or curvature map, was prepared from the total intensity maps. A nine-point square grid with a two-mile spacing was used (based on average depth to the magnetic basement), as well

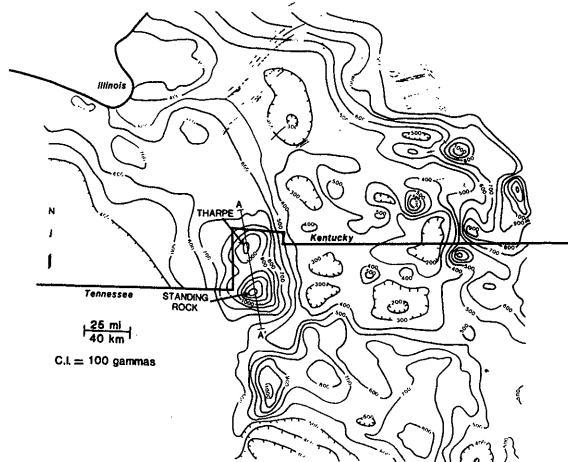


FIG. 1. Aeromagnetic map showing study area in Stewart County. A profile along A-A' is shown in Figure 2. This map is modified from a figure used in "The Adams, Tennessee magnetic anomaly" (Kemmerly, 1985).

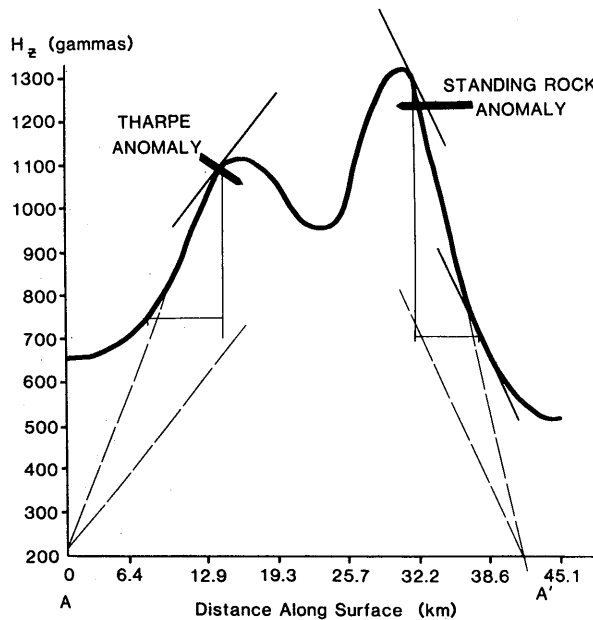


FIG. 2. Magnetic profile through line A-A' used for Peters half-slope analysis.

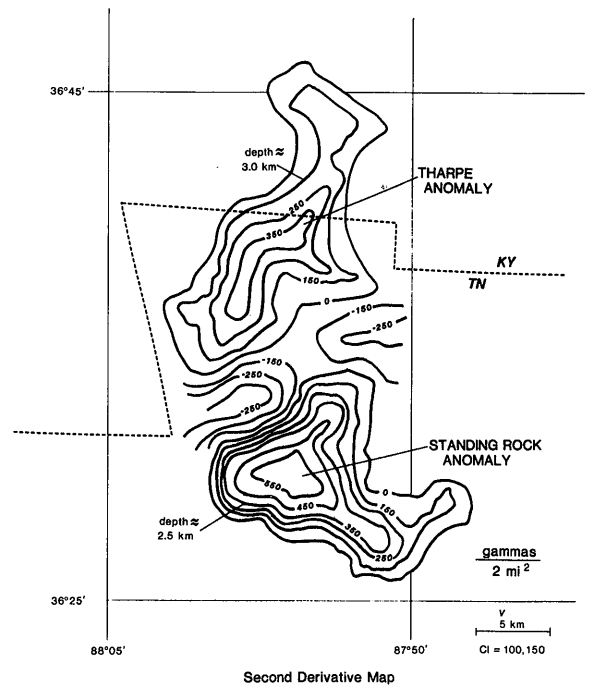


FIG. 3. Second derivative map of the Tharpe and Standing Rock anomalies.

as coefficients or "weighing factors" in a formula derived by Vacquier and others (1951). This grid system was applied over the entire study area, and the resulting numerical estimates of curvature were contoured (Figure 3). According to Vacquier and others (1951), the zero curvature line on the second derivative map approximates the planar geometry of the anomaly generating the rock body. Figure 4 reveals two large, asymmetric rock bodies. The Tharpe anomaly is a rock body measuring roughly 7.0 km by 22.0 km, with the long axis oriented N30° E. The Standing Rock anomaly measures approximately 8.0 km by 16.0 km, with a N60° W long-axis orientation.

MODELING

The use of the horizontal cylinder model with an average magnetic susceptibility of 2.5×10^{-3} emu gave the best approximation to the dimensions of the anomalies indicated on the curvature map. The susceptibility value was based on Hildenbrand's step model for the southeast margin of the Reelfoot rift (Hildenbrand, 1982). With this match to a theoretical model that is considerably longer in one dimension, the anomaly-causing bodies could be tentatively categorized as dikes.

DISCUSSION

From the analysis of depth to the magnetic basement it is found that the magnetic relief between the anomalies is 0.4 km. Generally the basement structure is sloping toward the northwest at about 7°, based on a vertical displacement of approximately 0.125 km per km of horizontal distance. This may reflect a gradual descent into the graben structure of the Reelfoot rift. The trend of the established southeastern margin of the rift extends in the direction of the present study area. Hildenbrand (1982) predicts a 20° slope in the magnetic basement along the southeastern

margin of the Reelfoot rift near Memphis, Tennessee. He also points out (in Hildenbrand and others, 1982) that the boundaries of the graben appear to widen as the rift extends northeast across western Kentucky. Some of the increase in rift width may be the result of block or listric normal faulting in the Tharpe-Standing Rock area.

The geophysical boundaries of the Reelfoot rift are associated with plutons emplaced in fissures resulting from normal faulting during the reactivation of the Reelfoot rift (Hildenbrand and others, 1982).

The Tharpe and Standing Rock anomalies are due to a contrast in magnetic susceptibility within the basement caused by either a lithologic or structural boundary. Their susceptibility value of 2.5×10^{-3} emu is close to the average value (2.59×10^{-3} emu) for basic igneous rock (Nettleton, 1976). The location and geophysical character of the Tharpe and Standing Rock anomalies suggest that they represent mafic intrusives associated with a down-dropped block along the Reelfoot rift margin.

LITERATURE CITED

- Hildenbrand, T. H. 1982. Model of the southeastern margin of the Mississippi Valley graben near Memphis, Tennessee, from interpretation of truck magnetometer data. *Geology*. 10:476-480.
- Hildenbrand, T.G., M.F. Kane, and J.D. Hendricks. 1982. Magnetic basement in the upper Mississippi embayment region—a preliminary report. In F.A. McKeown and L.C. Pakiser (eds.) *Investigations of the New Madrid, Missouri earthquake region*. U.S. Geological Survey Professional Paper #1236, pp. 39-53.
- Johnson, R.W., Jr., C. Haygood, and P.M. Kunselman. 1979. Residual total intensity aeromagnetic map of Tennessee: west-central sheet. Tennessee Division of Geology, Nashville, Tennessee.
- . 1978. Residual total intensity aeromagnetic map of Kentucky: western sheet. Kentucky Geological Survey, Lexington, Kentucky.
- Kemmerly, P.R. 1985. The Adams, Tennessee magnetic anomaly. *Journal of the Tennessee Academy of Science*. 60: no. 1, pp. 4-8.
- Nettleton, L.L. 1976. *Gravity and magnetics in oil prospecting*, New York: McGraw-Hill, 464 pp.
- Vacquier, V., N.C. Steenland, R.G. Henderson, and I. Zietz. 1951. Interpretation of aeromagnetic maps. *Geological Society of America Memoir* #47, 151 pp.

JOURNAL OF THE TENNESSEE ACADEMY OF SCIENCE

VOLUME 61, NUMBER 2, APRIL, 1986

NUCLEAR INVOLVEMENT IN MEMBRANE RECYCLING IN *ACANTHAMOEBA CASTELLANII*: AN ULTRASTRUCTURAL STUDY

GUS TOMLINSON

*Tennessee State University
Nashville, Tennessee 37203*

ABSTRACT

A new direction for membrane recycling viz., from nucleus to cytoplasm via a nuclear membrane budding process is reported for a small soil amoeba, *Acanthamoeba castellanii*. The outer smooth membrane of the nucleus is deposited into the cytoplasm after cells are induced to encyst. The deposited membrane may remain smooth or it may envelope cytoplasmic inclusions and become coated with dense particles which have the size, shape, density and staining properties of ribosomes. As encystment continues, the freshly deposited membrane may form canals between cytoplasmic inclusions and become deposited at the cell surface to become incorporated into the cyst wall.

INTRODUCTION

Recycling of membranes has been reported in mammals (Pelletier, 1973), amphibians (Heuser, 1973), and several types of Protozoa (Korn, 1974; Khaum, 1977; McKanna, 1973). While the cellular mechanisms involved in membrane recycling remain poorly understood, the direction of recycling based on reports to date is cell surface membrane to subcellular organelle viz., plasma membrane to pinocytotic or phagocytic vesicles in the cases of Protozoa or subcellular organelle membrane to another organelle membrane such as reuse of secretion vesicle membrane from synaptic transmission in mammals (Khaum, 1977; Bowers, 1980). Membranes do not remain static during recycling but undergo change as evidenced by alterations in particle distribution on fracture faces of recycled membranes examined by freeze-fracturing (Bowers, 1980). In addition, membrane recycling is not slow and sporadic. Quantitative studies on pinocytosis in *Acanthamoeba* showed that membrane recycling was continuous and rapid with a

quantity of cell membrane equivalent to the entire cell surface being recycled in a period of minutes (Bowers, 1972).

In this study, a new direction for membrane recycling is reported for *Acanthamoeba castellanii* viz., nuclear membrane recycled to the cytoplasm and eventually to the cell surface as the cell undergoes encystment.

MATERIALS AND METHODS

Culturing of the Organism

The experimental organism was *Acanthamoeba castellanii* which was grown in axenic culture. One liter of growth medium (GM) adjusted to pH 5.5 contained 10.0 g proteose peptone (Difco), 10.0 g glucose, 20.0 ml of 0.1 M phosphate buffer, 2.0 mg Ca⁺⁺, 20.0 mg Mg⁺⁺, 1 ug vitamin B₁₂, 1.0 mg vitamin B₁, and 0.1 ml of 0.01 M ferric citrate. The cultures were continuously aerated with air at the rate of 3 cu ft per hr per liter.

Log phase cells were induced to encyst synchronously by suspending them in an aerated culture of encystment medium (EM) consisting of 7.4 g KCl, 20 mg Mg⁺⁺, 2.0 mg Ca⁺⁺ and 20.0 ml of 0.1 M phosphate buffer. The solution was made up to 1 liter with H₂O and adjusted to pH 6.8 with NaOH.

Collection of samples for analysis

Samples were collected from a single culture of synchronously encysting cells as follows: A 3-liter culture of EM was adjusted to pH 6.8 and inoculated to a final concentration of 1.3×10^6 logphase cells per ml. The culture was aerated at 3 cu ft per hr per liter of EM. At zero time and at 2-hr intervals up to 36 hr, duplicate samples of 2.5×10^8 cells were removed aseptically and concentrated by centrifugation for subsequent fixation.

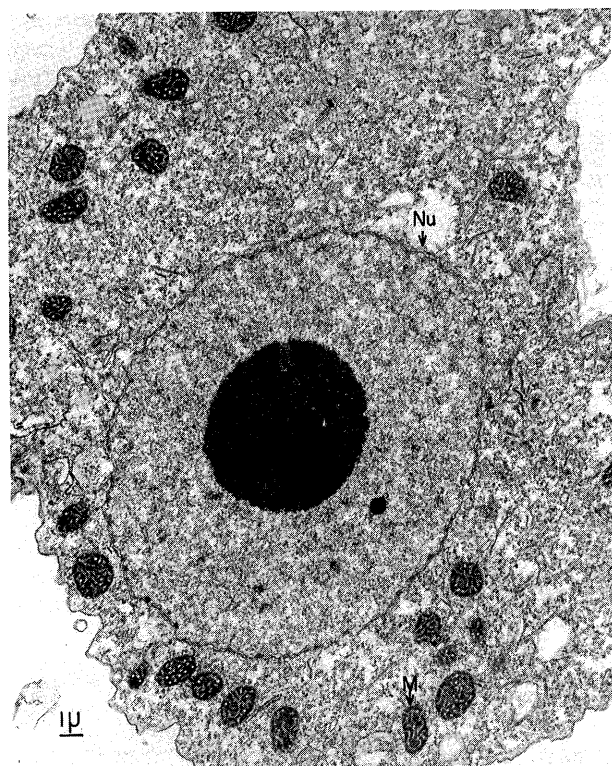


FIG. 1. Trophozoite *Acanthamoeba* showing a typical nucleus, N; mitochondrion, M; X 26,250.

Preparation for analysis by electron microscopy

Acanthamoeba were fixed for electron microscopy in 2% glutaraldehyde for 1 hour at 4°C and postfixed in 1% osmium tetroxide for 1 hour at 4°C. Specimens were dehydrated in ethanol using two washes of 50%, 70%, 95% and absolute, embedded in Epon 812 and sectioned on an LKB Ultratome with DuPont diamond knives. Specimens were then stained on grids with 1% uranyl acetate for 10 minutes and examined in a Philips 200 electron microscope operated at 40 KV to 100 KV with double conden-

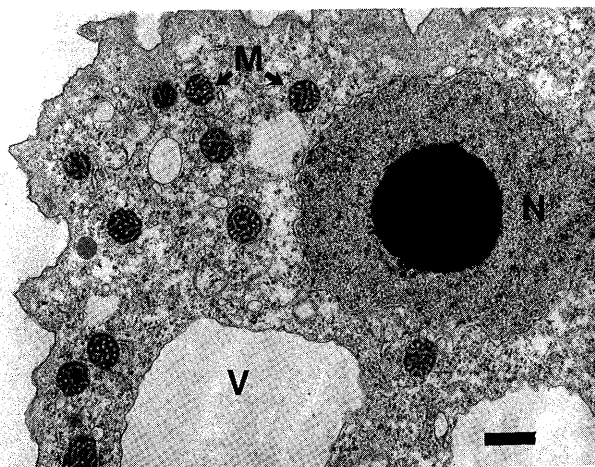


FIG. 2. *Acanthamoeba* at T₄ stage after induction to encyst. Nucleus, N; mitochondrion, M; vacuole, V; nuclear membrane, NM X 26,250.

sors and 20 micrometer molybdenum apertures in the objective lens.

RESULTS

Trophozoites of *Acanthamoeba* are characterized by a round or oval nucleus which is bordered by the classical, smooth double membrane and which encloses a single, conspicuous nucleolus. The cytoplasm is characterized by many granules, both free and membrane-bound, mitochondria with tubular cristae, many small vacuoles and an occasional lipid globule (Fig. 1).

When trophozoites of *Acanthamoeba* are induced to encyst, the two membranes of the nuclear envelope often begin to show greater than usual separation at many points around the nucleus. At this stage in preencystment, large contractile vacuoles form in the cytoplasm and cells become spherical in shape (Fig. 2).

By the T₈ stage of preencystment, both inner and outer nuclear membranes become heavily coated with dense granules and a nuclear budding process involving the outer nuclear membrane begins. During this process, smooth nuclear membrane is deposited into the cytoplasm where it often envelopes cytoplasmic inclusions and becomes coated with dense particles once again. The 30 nm particles, which coat the membranes both in the nucleus and the cytoplasm, possess the size, shape, density and staining properties of ribosomes (Fig 3). Sometimes particle-studded membrane forms connectors between cytoplasmic inclusions which have been enveloped by the nuclear budding process. In other instances the budded membrane appears smooth as it traverses the cytoplasm (Fig. 4).

As encystment proceeds, and cyst wall becomes visible at the periphery of the cell, fragments of smooth membrane can be seen as it becomes incorporated into the cyst

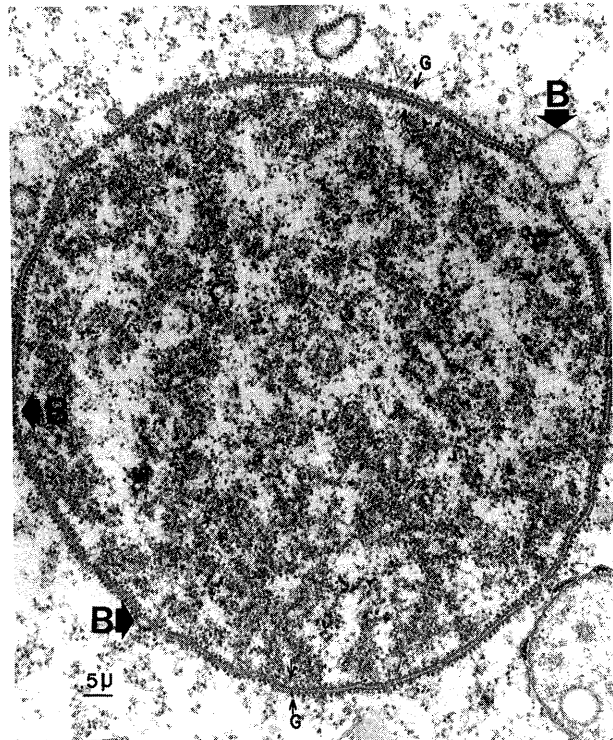


FIG. 3. *Acanthamoeba* nucleus at T₈ stage after induction to encyst. Granules, G; nuclear membrane bud, B X 70,000.

wall. Microtubules lie in close proximity and often lead to other large cytoplasmic vacuoles or other cytoplasmic inclusions (Fig. 5).

DISCUSSION

Recycling of cell surface membrane to pinocytotic and phagocytic vesicles and recycling of phagosome membrane to cell surface membrane is well documented for several cell types (See Introduction). Recycling of membrane derived from the nucleus to cytoplasmic organelles and subsequently into the framework of the cyst wall in *Acanthamoeba* adds a new dimension to the membrane recycling phenomenon. In this soil amoeba, encystment is a time of great change in membranes of the nucleus, cell surface, vesicles, vacuoles and tubules of the cell (Tomlinson, 1981). Added to this, encystment is often carried out under starvation conditions. Layering of old membrane or parts thereof at the cell surface to form very resistant cyst wall as a survival mechanism under environmental extremes of temperature, deprivation, desiccation or even attack by

other organisms may have endowed *Acanthamoeba* with great competitive capability and resistance under environmentally stressful conditions. This may explain why highly resistant bacterial endosymbionts of *Acanthamoeba* are often "trapped" in its cyst wall (Hall, 1985). Thus, the capacity for membrane recycling and reuse may have constituted an important evolutionary acquisition for this organism.

Nuclear membrane recycling during encystment in *Acanthamoeba* also correlates with formation of large masses of intranuclear actin microfilaments during cyst wall formation (Tomlinson, 1984; 1985). Not only contractile proteins but also enzymes necessary for their production, activation and inhibition are present in *Acanthamoeba* during encystment (Hammer, 1983; Kuznicki, 1984; Cote, 1985). Nuclear involvement in encystment may explain why profilin, a regulator of actin polymerization, is concentrated in the nucleus of *Acanthamoeba* (Tseng, 1984) and why actin filaments and capping protein are concentrated in the cortex near the cyst wall (Cooper, 1984).

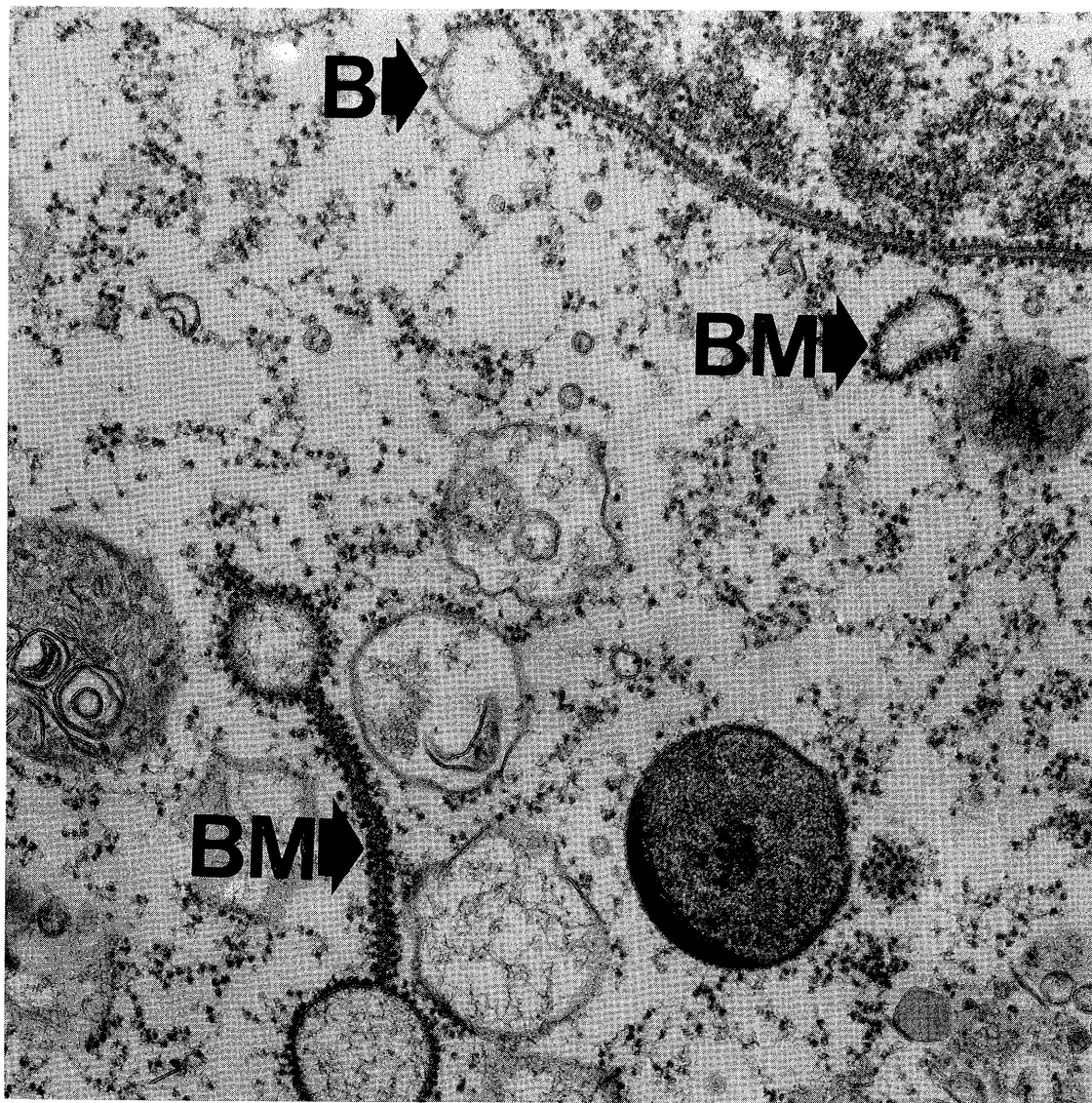


FIG. 4. *Acanthamoeba* at T_3 stage after induction to encyst. Nuclear membrane bud, B; bud membrane in cytoplasm, BM X 80,000.

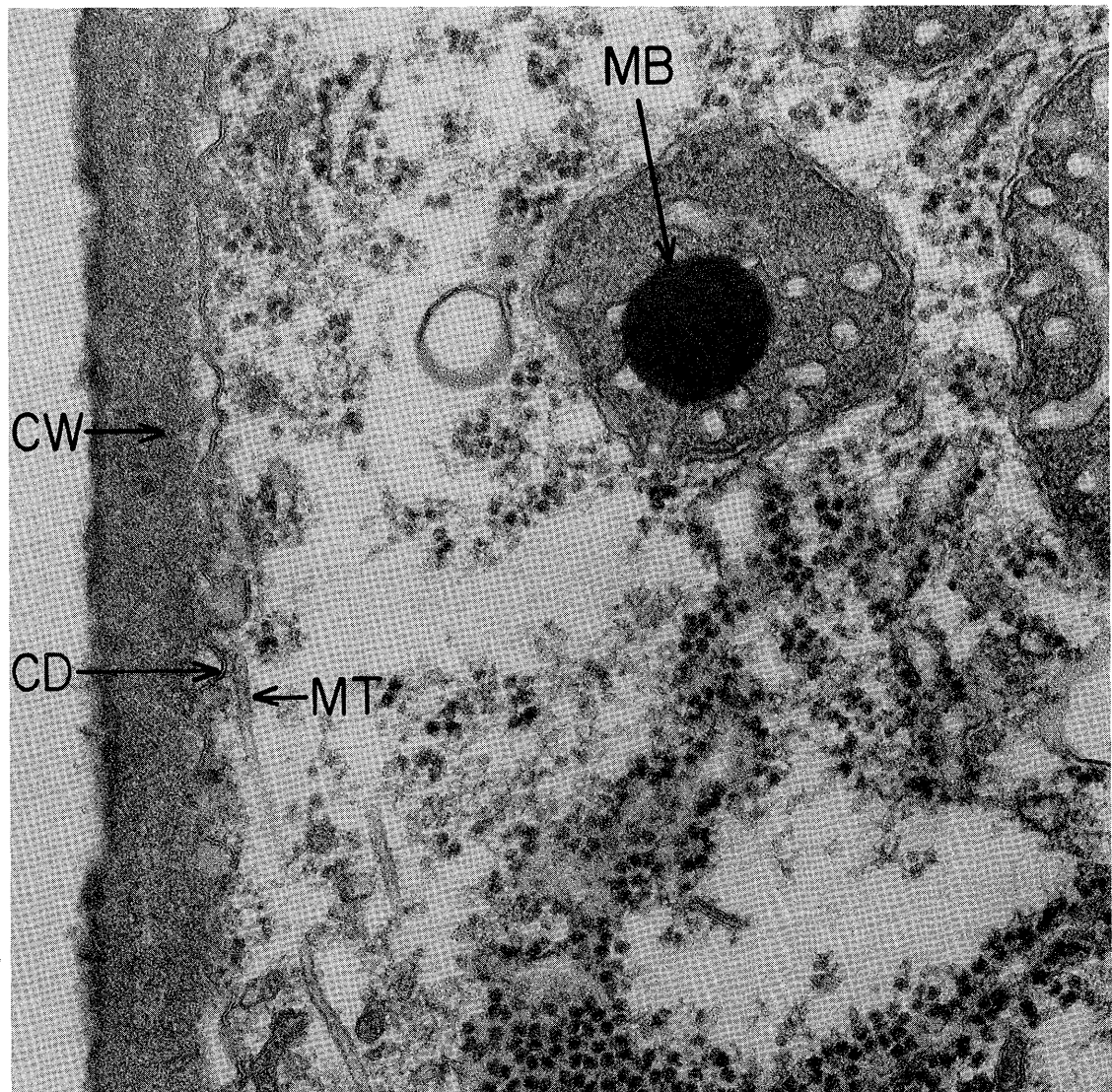


FIG. 5. Young *Acanthamoeba* cyst at T_{24} stage after induction to encyst. Cyst wall, CW; microtubule, MT; mitochondrial body, MB; cyst wall deposition of budded membrane, CD X 80,000.

REFERENCES CITED

- Bowers, B. 1977 Comparison of pinocytosis and phagocytosis in *Acanthamoeba castellanii*. *Exp. Cell Res.* 110 409-417.
- Bowers, B. and T. E. Olszowski. 1972 Pinocytosis in *Acanthamoeba castellanii*. *J. Cell Biol.* 53 681-694.
- Bowers, B. 1980 A morphological study of plasma and phagosome membranes during endocytosis in *Acanthamoeba*. *J. Cell Biol.* 84 246-260.
- Cooper, John A., J. D. Blum and T. D. Pollard. 1984 *Acanthamoeba castellanii* capping protein, Properties, mechanism of action, immunologic cross-reactivity and localization. *J. Cell Biol.* 99 217-225.
- Cote, G. P., J. P. Albanesi, T. Ueno, J. Hammer and E. Korn. 1985 Purification of low-molecular weight myosin that resembles myosin I from *Acanthamoeba castellanii*. *J. Biol. Chem.* 260 (8) 4543-46.
- Hall, John and H. Voeltz. 1985 Bacterial endosymbionts of *Acanthamoeba*. *J. Parasit.* 71 (1) 89-95.
- Hammer, John, J. Albanesi, and E. Korn. 1983 Purification and characterization of a myosin I heavy chain kinase from *Acanthamoeba castellanii*. *J. Biol. Chem.* 258 (16) 10168-75.
- Heuser, J. and T. Reese. 1973 Evidence for recycling of synaptic vesicle membrane during transmitter release at the frog neuromuscular junction. *J. Cell Biol.* 57 315-44.
- Khaun, Y. and G. Thompson. 1977. Differentiation of food vacuolar membranes during endocytosis in *Tetrahymena*. *J. Cell Biol.* 75 436-45.
- Kuznicki, J. and E. Korn. 1984 Interdependence of factors affecting the actin-activated ATPase activity of myosin II from *Acanthamoeba castellanii*. *J. Biol. Chem.* 259 (14) 9302-07.
- Korn, E., B. Bowers, S. Baezri, and S. Simmons. 1974 Endocytosis and exocytosis: Role of microfilaments and phospholipids in membrane fusion. *J. Supramol. Struct.* 241 528.
- McKanna, J. A. 1973 Cyclic membrane flow in the ingestive system of peritrich protozoans. *J. Cell Sci.* 13 663-75.
- Pelletier, G. 1973 Secretion and uptake of peroxidase by hypophyseal cells. *J. Ultrastruct. Res.* 43 445-49.
- Spies, F., A. Linnemann and P. Elbers. 1975 Encystment of *Acanthamoeba castellanii*: combined freeze etch-thin sectioning of cell surface. *Cytobiologie* 11 50-64.
- Tomlinson, G. 1981 Nuclear changes in *Acanthamoeba* during encystment. *J. TN Acad. Sci.* 56 (3) 107-08.
- Tomlinson, G. 1984 Intranuclear microfilaments and cellulose synthesis in *Acanthamoeba*. *J. TN Acad. Sci.* 59 (4) 90-92.
- Tomlinson, G. 1985 Sequential induction of mitochondrial changes during encystment in *Acanthamoeba castellanii*. *J. TN Acad. Sci.* 60 (4) 95-97.

ACKNOWLEDGMENT

This research was supported by funds provided by NIH Grant 2 SO6 RR 08092 - 12.